BIOCHEMISTRY
including biophysical chemistry & molecular biology

Article

pubs.acs.org/biochemistry

Crystal Structures of *Escherichia coli* Branching Enzyme in Complex with Linear Oligosaccharides

Lei Feng,[†] Remie Fawaz,[†] Stacy Hovde,[†,‡] Lindsey Gilbert,[†] Janice Chiou,[†] and James H. Geiger*[,†]

[†]Department of Chemistry, Michigan State University, East Lansing, Michigan 48824, United States

[‡]Department of Biochemistry and Molecular Biology, Michigan State University, East Lansing, Michigan 48824, United States

Supporting Information

ABSTRACT: Branching enzyme is responsible for all branching of glycogen and starch. It is an unusual member of the α-amylase family because it has both α-1,4-amylase activity and α-1,6-transferase activity [Drummond, G. S., et al. (1972) *Eur. J. Biochem. 26*, 168−176]. It also does not react with shorter glucans, though it will bind much longer substrates and substrate mimics [Binderup, K., et al. (2002) *Arch. Biochem. Biophys. 397*, 279−285]. In an effort to better understand how branching enzyme interacts with its polymeric substrate, we have determined the structure of Δ112 *Escherichia coli* branching enzyme bound to maltoheptaose and maltohexaose. Together, these structures define six distinct oligosaccharide binding sites on the surface of *E. coli* branching enzyme. Most of these binding sites surround the edge of the β-barrel domain and are quite far from the active site. Surprisingly, there is no evidence of oligosaccharide binding in the active site of the enzyme. The closest bound oligosaccharide resides almost 18 Å from the active site. Mutations to conserved residues in binding sites I and VI had a debilitating effect on the activity of the enzyme.

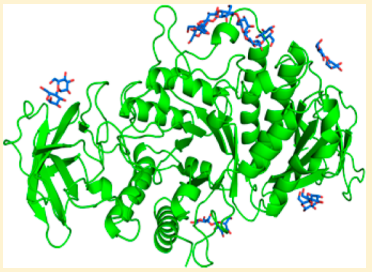

Starch is one of the most useful, easily produced, and versatile renewable products known. More than 1 billion tons of starch is consumed annually, providing the majority of caloric intake for humans and animals, a biodegradable feedstock for a variety of industrial applications, and a renewable source of transportation fuels. There has been significant recent interest in altering the properties of starch to produce a biomaterial better suited for its various applications.[1−7] It is therefore critical to understand the structure, function, and specificity of the enzymes responsible for starch biosynthesis and modification.

Starch and glycogen are the storage carbohydrates of all organisms from bacteria to humans. They both consist of glucose polymers formed predominantly by α-1,4 linkages. However, a significant percentage of the material is branched at the 1,6 position, which is critical for the structure, function, and bioavailability of starch and glycogen.[6] While glycogen is more or less homogeneous, starch consists of two different polymers, amylose, consisting almost entirely of linear chains of smaller polymers, and amylopectin, which consists of much larger polymers that are 2−3% branched at the 1,6 position. Branching enzymes (BEs) are responsible for the formation of these branch points.

While most bacteria and other eukaryotes have only a single isoform of branching enzyme (BE), virtually all plants have three BE isoforms, BEI, BEIIa, and BEIIb. These isoforms differ in their temporal expression, specificity, substrate specificity, and product.[8−13] While BEII isoforms tend to produce shorter chain branches with six or seven glucose units, BEI favors the transfer of much longer oligomers with 14−70 units.[12,14,15] The isoforms of plant BEs are proposed to play distinct roles in the formation of the complex starch granule, at least in some species.[8] The bacterial BEs catalyze the identical reaction and also manifest branch chain specificity. Biochemical analysis of bacterial enzymes has shown that BEs can have very distinct branch chain specificities depending on the bacterial species.[16−20] It has also been suggested that bacteria make distinct forms of glycogen depending on their environment. Bacteria like Enterobacteria, which live primarily in other organisms where food is relatively plentiful, tend to have glycogen made up of longer average glucan chains, while organisms that must survive for extended periods outside of a host, in relatively hostile environments, tend to produce glycogen with much shorter average glucan chains. While glycogen with longer chains is broken down more rapidly, shorter chain glycogen is consumed more slowly, allowing the organism to survive, at a slower rate of metabolism, for much longer in the absence of food. It is possible that the specificity and reactivity of BE are important in controlling the type of glycogen produced by a given organism. Therefore, BE is proposed to play an important role in tailoring an organism's storage of glucan for optimal breakdown, in both plants and animals.[21]

BE belongs to the glycosyl hydrolase GH13 family of enzymes (http://www.cazy.org/). These include α-amylases, isoamylases, cyclodextrin glucanotransferases, pullulanases, and almost all branching enzymes,[22−28] though a few GH57 BEs have recently been identified.[29] All GH13 family members

Received: March 3, 2015
Revised: July 23, 2015
Published: August 17, 2015

DOI: 10.1021/acs.biochem.5b00228
Biochemistry 2015, 54, 6207−6218

share the α/β_8 "TIM barrel" fold that contains the enzyme active site. In addition, the active sites of all of the enzymes in the family are also very similar, highlighted by the presence of two acidic residues that are absolutely conserved in all enzymes of the family. The mechanism of all of the family members is also thought to be quite similar, consisting first of cleavage of an α-1,4-glucan linkage by nucleophilic attack by the carboxylate nucleophile to form an enzyme/substrate covalent intermediate, followed by a second nucleophilic attack by the acceptor nucleophile to yield the product with overall retention of configuration.[30−32] Though many of the GH13 enzymes act on the same substrate, an α-1,4-glucan polymer, the products differ on the basis of the identity of the acceptor. While water is the acceptor for the amylases, a sugar hydroxyl group is the acceptor for the glucanotransferases such as cyclodextrin glucanotransferase (CGTase) and BE. A recent directed evolution study has shown that a CGTase can be converted into an α-amylase with only three amino acid changes, all of which are in the acceptor glucan binding site,[33] indicating that controlling acceptor binding is sufficient to control the reaction catalyzed by the enzyme in some cases. BE differs from most of these enzymes in that it is not inhibited by short chain glucan mimics such as acarbose, a four-unit complex oligosaccharide containing an acarviose unit. Given that BEs vary in the length of the glucan chain transferred, often transferring glucans no shorter than hexaose and preferring the transfer of much longer glucans,[34,35] it would therefore appear that branching enzymes differ from most of their family members in that relatively large reactants are required, and only relatively large glucans can be transferred. This introduces a unique problem in enzymology in that substrate binding must somehow be distributed over a relatively large molecular substrate surface to achieve such specificity.

The N-terminal truncation of 112 residues in *Escherichia coli* BE was reported to retain 40−60% branching activity compared to that of the wild-type protein (*wt*EcBE).[36] The structure of the truncated *E. coli* BE was the first BE structure determined (this truncated BE will be termed EcBE throughout).[37] This structure showed that the domain architecture of the enzyme was very similar to that of isoamylase, an enzyme that cleaves the α-1,6-linkage of malto-oligosaccharides and revealed an N-terminal β-sandwich domain later defined as a carbohydrate binding module 48 domain, a central $(\beta/\alpha)_8$ barrel catalytic domain shared by all GH13 enzymes, and a C-terminal β-sandwich domain shared by α-amylases and other members of the GH13 family.[37] Inspection of the EcBE structure gives no clue about the substrate specificity as the substrate binding region defined in the structures of other GH13 enzymes is quite different in EcBE.[37] A structure of BE from *Mycobacterium tuberculosis* revealed the N-terminal domain to be structurally similar to the CBM48 domain. Removal of this N-terminal domain was required to obtain well-diffracting crystals of *E. coli* BE.[38] Even more recently, structures of SBEI from rice were determined both alone and bound to maltopentaose and showed that plant BEs do not share the N-terminal domain seen in the bacterial BEs.[39,40] Three maltopentaose binding sites were identified in rice SBEI, all quite far from the active site.

In an effort to better understand reactant and product specificity in EcBE, we have determined the structures of EcBE bound to maltohexaose (M6) and maltoheptaose (M7). These structures suggest a mechanism by which EcBE may select for its relatively long substrates and products.

MATERIALS AND METHODS

Protein Preparation. The recombinant EcBE was overexpressed and purified (>95% pure by sodium dodecyl sulfate−polyacrylamide gel electrophoresis) as previously described.[37,41] The protein was concentrated to 10 mg/mL in a buffer solution containing 25 mM HEPES (pH 7.5) and 10% glycerol. The wild-type full-length and truncated proteins used for the iodine stain assay were obtained in a manner different from that described above. The DNA sequences encoding both *wt*EcBE and EcBE were engineered into a modified pET28 vector containing histidine and Sumo[42] tags to make the vectors designed as follows: His-Sumo-*Bam*HI-EcBE-*Sal*I and His-Sumo-*Bam*HI-*wt*EcBE-*Hin*dIII. Mutations of *wt*EcBE and EcBE were all performed using these vectors. The vectors were then transformed into BL21(DE3) cells (purchased from EMD Millipore). The cells were grown in LB medium and overexpressed with 0.5 mM IPTG at 25 °C for 5 h at an OD_{600} of 0.5 before being centrifuged and frozen at −20 °C. The cells were lysed by sonication in lysis buffer [100 mM NaCl, 1 mM BME, and 50 mM Tris (pH 8.0)] and 10 mM imidazole. The *wt*EcBE lysis buffer had 20 mM Tris (pH 7.5) as the buffering component. The cell debris was removed by centrifugation (9000 rpm, SS-34 rotor) for 30 min. The soluble extract was loaded onto a Ni-NTA affinity resin (purchased from Qiagen) in lysis buffer, and the column was washed with lysis buffer and 30 mM imidazole to remove nonspecifically bound impurities. In the case of EcBE, the N-terminal tag was removed using the Sumo protease (0.03 mg for 2 h) on the column, and the proteolyzed protein eluted in lysis buffer. In the case of *wt*EcBE, the protein was eluted from the Ni-NTA resin using lysis buffer and 250 mM imidazole and then digested overnight using the Sumo protease while being dialyzed against lysis buffer without imidazole.

Malto-Oligosaccharide-Bound EcBE Crystals Generated by Substrate Soaking. The final purified EcBE protein was buffer exchanged into 25 mM Na-Hepes (pH 7.5) and concentrated to ∼10 mg/mL. Crystals were grown as previously described.[37] The crystals reached their optimal size after 2 months. The oligosaccharides were prepared in solutions containing 100 mM Na-Hepes (pH 7.2). The apoenzyme crystals were directly transferred into the oligosaccharide solutions at 277 K for the maximal time period before crystal cracking was visually evident. The crystals were then cryoprotected and flash-frozen in liquid nitrogen as previously described for the apoenzyme.[37] Table 1 lists the maximal soak times and oligosaccharide concentrations for which diffraction quality data could be obtained.

Table 1. Summary of Oligosaccharide[a] Soaking Conditions

substrate	MW (Da)	soaking concentration (mM)[64]	soaking time (h)	malto-oligosaccharide electron density?[b]
maltose	342	200	72	no
maltotriose	504.4	100	72	no
maltotetraose	666.6	140	12	no
maltopentaose	828.7	100	6	yes
maltohexaose	990.9	50	3	yes
maltoheptaose	1153	90	3.5	yes

[a]All oligosaccharides were purchased from Sigma. [b]Indicates whether electron density for the oligosaccharide resulted from data collected from soaked crystals.

DOI: 10.1021/acs.biochem.5b00228
Biochemistry 2015, 54, 6207−6218

Data Collection, Processing, and Structural Refinement. The X-ray diffraction data were collected at LS-CAT, sector 21, at the Advanced Photon Source. At least 200° of data were collected using 1° oscillations. Diffraction data were indexed, integrated, and scaled using the HKL2000 software package.[43] The molecular replacement program MOLREP was used to position the apo EcBE structure [Protein Data Bank (PDB) entry 1M7X] in each case, and REFMAC5 was used to refine the structure.[44] Table 2 lists the refinement statistics for the branching enzyme/oligosaccharide complex structures. The lack of completion at high resolution for the M7-bound structure is due to minor anisotropy in the diffraction pattern as the data are virtually complete at lower resolution. Coordinates and structure factors have been deposited in the PDB as entries 4LQ1 and 4LPC.

Table 2. X-ray Data Collection and Refinement Statistics of *E. coli* BE/Oligosaccharide Complexes

	E. coli BE/M6	*E. coli* BE/M7
Structural Data		
space group	$P2_1$	$P2_1$
no. of molecules per asymmetric unit	4	4
total no. of atoms	20219	20728
no. of water molecules	553	842
ligands	maltohexaose, glycerol	maltoheptaose, glycerol
unit cell parameters		
a, b, c (Å)	93.7, 104.1, 186.7	92.2, 103.4, 185.9
α, β, γ (deg)	90, 91.85, 90	90, 91.57, 90
wavelength of X-ray (Å)	0.9785	0.9785
resolution (Å)	2.55	2.39
total no. reflections	111798	138111
completeness (%)	96.3 (97.1)	90.4 (86.9)
multiplicity	3.7 (3.7)	4.3 (4.3)
I/σ	29.4 (4.18)	23.3 (3.3)
R_{merge} (%)	8.0 (43.9)	9.1 (54)
Refinement Statistics		
R_{work} (%), R_{free} (%)	17.79, 22.38	18.3, 23.4
B factor	75	60
rmsd for bond lengths (Å)	0.010	0.011
rmsd for bond angles (deg)	1.240	1.338
PDB entry	4LQ1	4LPC

Branching Enzyme Activity Assay. The iodine stain assay was used to compare the activity of wild-type and mutant enzymes.[45] The absorbance of the glucan−iodine complex is decreased by the activity of the branching enzyme on the substrate amylose [potato type III (dp 1176, chain length 884, Sigma Scientific)]. Reaction mixtures contained, in a final volume of 500 μL, 50 mM citrate (pH 7.0) and 0.1 mg of amylose. The reaction was initiated by the addition of an appropriate amount of enzyme. One unit of activity is defined as the decrease in absorbance of 1.0 per minute at 30 °C at 660 nm.

RESULTS

Both cocrystallization and crystal soaking experiments were conducted using a variety of oligosaccharides with EcBE, including maltose, maltotriose, maltotetraose, maltopentaose, M6, and M7 at a variety of concentrations. Cocrystallization with maltose resulted in crystals, but no maltose binding could be identified in the resulting electron density map. Cocrystallization attempts with all other malto-oligosaccharides failed to produce crystals. Soaking experiments with all oligosaccharides, with the exeption of maltose, resulted in crystal cracking at higher concentrations. Carefully screening both concentration and time resulted in crystals of EcBE soaked in all the malto-oligosaccharides. However, again no electron density for maltose was detected. Density suggestive of weak binding was observed in some binding sites for maltotriose, maltotetraose, and maltopentaose, but in none of these cases was the density interpretable. However, soaking experiments with both M6 and M7 resulted in electron density of sufficient quality to build oligosaccharides, with the density for M7 the most complete and well-occupied. Figure S1 shows electron density for the bound glucans in each of the six binding sites. In general, the longer the oligosaccharide, the more evidence of binding. However, only the M6- and M7-bound EcBE structures are reported here.

The overall structure of malto-oligosaccharide-bound EcBE is virtually identical to that of apo EcBE previously determined,[37] with only minor, local conformational changes caused by the binding of the oligosaccharides. The crystal form used in soaking experiments is also identical to that of the apo structure and contains four distinct molecules in the asymmetric unit, labeled A−D, the same labeling used for the apo EcBE structure.[37] Crystal packing interactions prevent occupancy of all oligosaccharide binding sites in all four molecules. Overall, six distinct binding sites have been identified in the two structures. The composite structure in Figure 1a shows all six binding sites. Interestingly, and consistent with biochemical data that show no reaction or inhibition with shorter oligosaccharides or oligosaccharide derivatives such as acarbose, no oligosaccharide binding is detected in the active site. This is in contrast with virtually all other GH13 protein/oligosaccharide complex structures known, which all show active site binding. This may indicate that EcBE has substantially less affinity for shorter oligosaccharides in its active site than do other enzymes in the family. Table 3 summarizes the occupancy of each site in each of the two structures. The six binding sites can be divided into three general categories on the basis of their location relative to the active site. Binding sites I, II, and IV are all located on the "top" edge of the enzyme, and on the side of the active site where the nonreducing end of the donor glucan is expected to exit. Binding site V is also on the top edge of the enzyme, bridging the catalytic and C-terminal domains. Binding sites III and VI are located on the "bottom" of the enzyme and are in the vicinity of where the reducing end of the glucan would emerge from the active site. This expectation is borne out by every GH13 enzyme/oligosaccharide structure known, all of which show the nonreducing end of the glucan emanating in this direction.[27,46−49] To illustrate this point, Figure 1b shows an overlay of the composite EcBE structure with the oligomers from pullulanase (PDB entry 2FHF) bound in the active site modeled in EcBE.

M6 and M7 Binding to Sites I and II. Binding sites I and II are approximately 20 Å from the active site. In molecule B, a tetraose molecule occupies binding site I and a maltose is visible in binding site II (Figure 2a,b). The two glucose units on the nonreducing end of site I (sugars 1 and 2) interact with the protein, while the other two units (sugars 3 and 4) arch away from this site and point toward site II. Both glucose units visible in site II (sugars 1 and 2) interact with the protein (Figure 2b). The oligosaccharides seen in these two binding sites seem to come from a single M7 molecule, but the density for the sugar

DOI: 10.1021/acs.biochem.5b00228
Biochemistry 2015, 54, 6207−6218

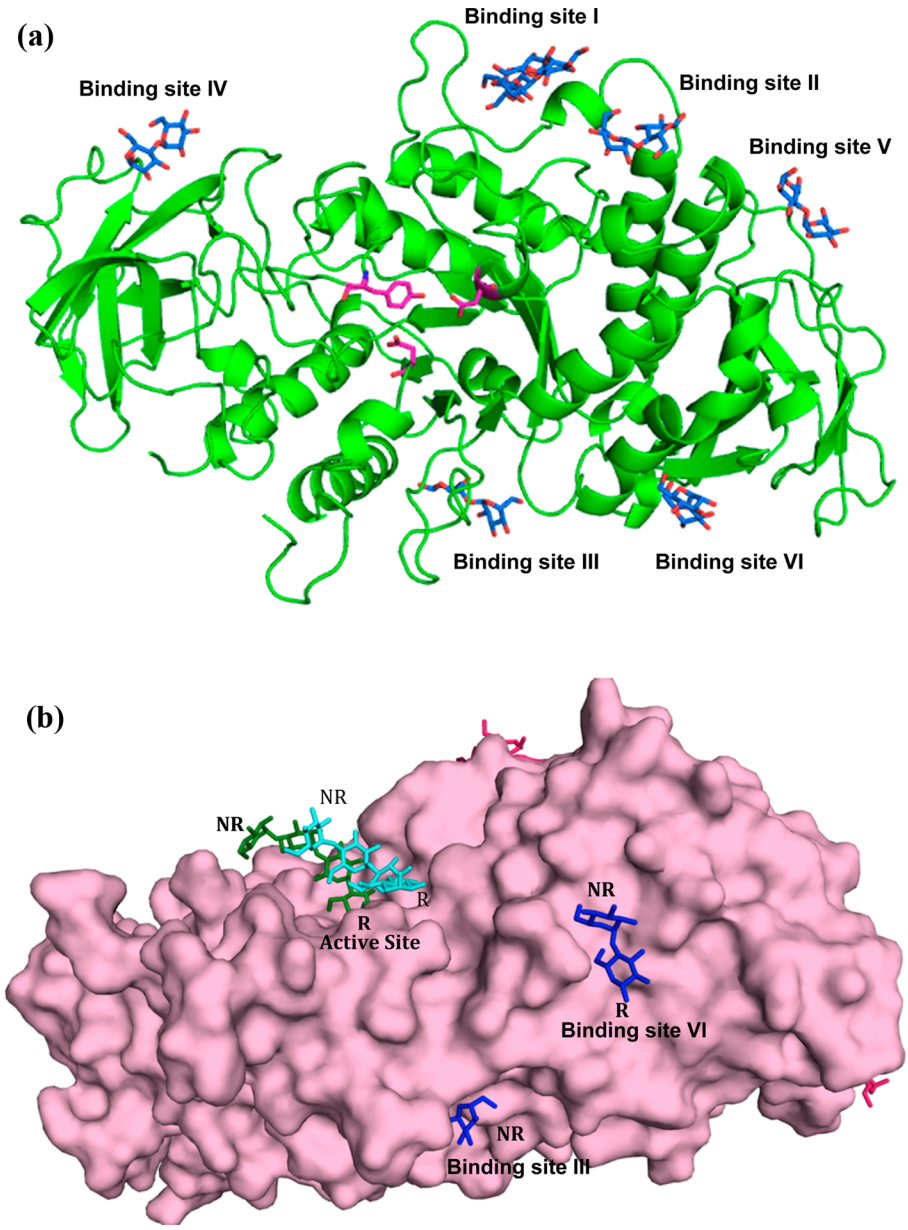

Figure 1. (a) Composite view of the linear oligosaccharide binding sites in EcBE. The figure was made by first overlaying all four molecules in the asymmetric unit and showing the malto-oligosaccharides in each binding site on EcBE molecule B (green cartoon) to show the relative positions of the six binding sites (colored by atom, with C colored marine and O colored red). The oligosaccharides shown in sites I–III and VI are from molecule B; the oligosaccharides shown in site IV are from molecule D, and the oligosaccharide shown in site V is from molecule C. Three active site residues (Tyr300, Asp335, and Asp526) are also shown (colored magenta). (b) Malto-oligosaccharides from *Klebsiella pneumoniae* pullulanase (colored forest green and cyan) are modeled into the active site of EcBE (light pink), showing how binding sites III and VI (blue) are located on the external surface of the molecule where the active site oligosaccharides are expected to exit. Two other oligosaccharides from binding sites III and VI are colored pink. The reducing (shown with R) and nonreducing (shown with NR) ends are also labeled for each oligosaccharide.

that bridges the binding sites is very weak and uninterpretable (sugar 5, not shown in figures).

Binding site I makes several hydrogen bonds with sugars 1 and 2. Hydrogen bonds are formed between O2 of glucose 1 and the side chain of Glu590 and between O6 of glucose 1 and the main chain and side chain of Arg255 and Ser583, respectively. Together, these interactions serve to define this site as being specific for the nonreducing end. Hydrogen bonds are also made between O2 of glucose 2 and the side chains of Arg576, Asp585, and His587, between the side chain and main chain of His587 and O3 of glucose 2, and finally between NH1 of Arg254 and O4 of glucose 1. In addition, hydrogen bonds are made between the side chain of Arg576 and O5 of Glu3 and O3 of Glu4, serving to direct the trajectory of the glucan as it exits binding site I. An unusual, end-on hydrophobic interaction is also made between Trp586 and glucose 1. Though virtually all of these residues are conserved in Enterobacteria, they are not conserved in bacteria from other families (Figures S2 and S3[50]). Essentially identical interactions between the first two glucose units and EcBE are seen in three of the four molecules of the asymmetric unit (A, B, and D), though more of the glucan chain is visualized in molecule B. In molecule D, electron density for two more glucose units can be seen, but the trajectory of the two glucose units is distinct from that seen in

DOI: 10.1021/acs.biochem.5b00228
Biochemistry 2015, 54, 6207–6218

Table 3. Binding Sites in *E. coli* BE/Linear Oligosaccharide Complex Structures

binding site	location	subunits occupied	residues
I	nonreducing end, bridging oligo, catalytic domain	A–D (M6)	Arg254, Arg255, Arg576, Ser583, Leu584, Asp585, Trp586, His587, and Glu590
		A, B, and D (M7)	
II	reducing end, bridging oligo, catalytic domain	B and D (M7)	Asp537, Lys546, Trp595, and His596
III	catalytic domain, bottom of barrel	A and B (M7)	Arg468, Pro469, Leu475, Gly476, Phe477, Trp478, and Asn518
IV	N-terminal domain	B (M7)	Trp159, Lys189, Leu201, Gln211, and Glu215
		D (M6 and M7)	
V	bridging catalytic and C-terminal domains, "top side"	C (M6 and M7)	Asp542, Trp544, Gln545, Pro659, Pro661, and Ser689
VI	bridging catalytic and C-terminal domains, "bottom side"	A and B (M7)	Thr508, Phe509, Leu512, and Trp628

B, where the glucan chain also interacts with binding site II (Figure 2c, overlay of molecules D and B). In molecule D, the glucan chain points away from the surface of the enzyme and binding site II. The differences in M7 trajectory are probably determined by binding of the reducing end of the sugar to binding site II.

Binding site II interacts with a maltose. Binding to this site is seen only in molecule B of the M7-bound complex. O3 and O6 of glucose 7 make hydrogen bonds to the side chains of His596 and Lys546, respectively, while in sugar 6, O2 makes hydrogen bonds with the Asp537 and Lys546 side chains and O3 with the side chain of Asp537 to complete the binding interactions that serve to stereochemically define binding site II as a reducing end binding site. Binding site II is far more weakly conserved, with only two residues (K546 and F547) strongly conserved in bacteria, and none of the residues conserved in the eukaryotic enzymes (Figures S2 and S3). In addition, inspection of the structure of rice SBEI (Figure 2d) shows that this binding site is filled by a short helix that is not present in EcBE, MtBE, or, apparently, any of the other bacterial BEs.

M6 also appears to occupy both binding sites I and II, but density for most of the oligosaccharide is quite weak. Two glucose moieties can be modeled in binding site I, but the rest of the electron density is too weak to interpret. It appears that M6 is not of sufficient length to bridge the two sites and is therefore only seen well-bound in the presumably better binding site I.

M6 and M7 Binding to Sites III–VI. Four other oligosaccharide binding sites were also identified in both the M6/EcBE and M7/EcBE structures. In each case, only two glucose units are visible in the binding sites with the remainder of the oligosaccharide disordered. Sites III and VI are located near where the reducing end of the glucan typically exits a GH13 enzyme (Figure 1b).[47] Site III is defined by only three hydrogen bond interactions between EcBE and two glucose units of M7: The main chain carbonyls of Gly476 and Phe477 make hydrogen bonds with O5 and O6 of the sugar on the reducing end of the maltose unit, respectively, and the Arg468 main chain nitrogen makes a hydrogen bond with O6 of the reducing end sugar (Figure 3a).

There are also numerous hydrophobic interactions between the maltose unit visible in the electron density and Phe239, Trp478, and Pro469, with the former two making classic sugar/aromatic stacking interactions.[51] The site is also occupied in the A chain, where both visible glucose units make similar interactions with EcBE. This site displays relatively strong conservation across species in many positions. Pro469, Leu475, Gly476, and Phe477 are conserved in all species, from bacteria to humans (Figures S2 and S3). While Trp478 is not conserved, a His (His453 in MtBE and His388 in SBEI, equivalent to Gly447 in EcBE) occupies a similar position in both the MtBE and SBEI structures (Figure 3b). This His is conserved in all eukaryotic BEs and is an aromatic residue in virtually all bacterial BEs. However, maltopentaose is not bound in this site in the SBEI/maltopentaose structure.

Binding site IV is in the N-terminal, CBM48 domain and is located on the same face of the enzyme as are binding sites I and II (Figure 1a). It is characterized by hydrogen bonding interactions, three to the nonreducing maltose unit (the side chain of Gln211 to O2 and O3 and the side chain of Glu215 to O3) and one to the reducing end sugar of the maltose fragment (the side chain of Lys189 to O2) (Figure 4a). There is also a classic sugar/aromatic stacking interaction involving Trp159 and the reducing end sugar. The maltose unit is comparatively undistorted in this binding site. Two residues, Trp159 and Lys189, are absolutely conserved in all branching enzymes, and a Glu replaces Gln211 in all other bacterial BEs (Figures S2 and S3). Though not conserved in plants, Lys121 in SBEI occupies the position occupied by the Gln211 side chain, and this residue is absolutely conserved in the plant enzymes (Figure 4b). Only three other structures of a glucan-bound CBM48 domain are available, the 5′-AMP-activated protein kinase β subunit bound to β-cyclodextrin (PDB entry 1Z0M), starch phosphatase DSP4 (PDB entry 4PYH), and maltopentaose-bound starch branching enzyme 1 (PDB entry 3VU3), though there is only a single glucose unit visible in the binding site in the latter structure.[52,53] Figure 4c displays an overlay of the CBM48 domains of EcBE, the human AMP-activated protein kinase β subunit (AMPK) and the starch phosphatase DSP4 and shows that Trp159 and Lys189 make similar interactions with the glucans in the two structures, despite large differences in the sequences of the three proteins, and in the structure of the glucan bound (linear malto-saccharides vs β-cyclodextrin). This indicates that many CBM48 domains may bind glucans similarly, which is not always seen with the relatively promiscuous binding of CBM domains.

Two binding sites, binding sites V and VI, bridge the catalytic and C-terminal domains. Binding site V is also on the same face of the molecule as binding sites I, II, and IV. Similar to binding site IV, binding site V is also characterized by a stacking interaction between a surface-exposed tryptophan residue (Trp544) and the reducing end of the maltose unit (Figure 5a). Two hydrogen bonds are made to the reducing end sugar (the Asp542 side chain to O2) and three to the nonreducing end sugar moiety (the main chain carbonyl of Pro659 to O2 and O3 and the side chain of Ser689 to O6). Binding site VI is found on the opposite side of the molecule from binding site V (Figure 5b). Though found in molecules A, B, and D, it is best

DOI: 10.1021/acs.biochem.5b00228
Biochemistry 2015, 54, 6207–6218

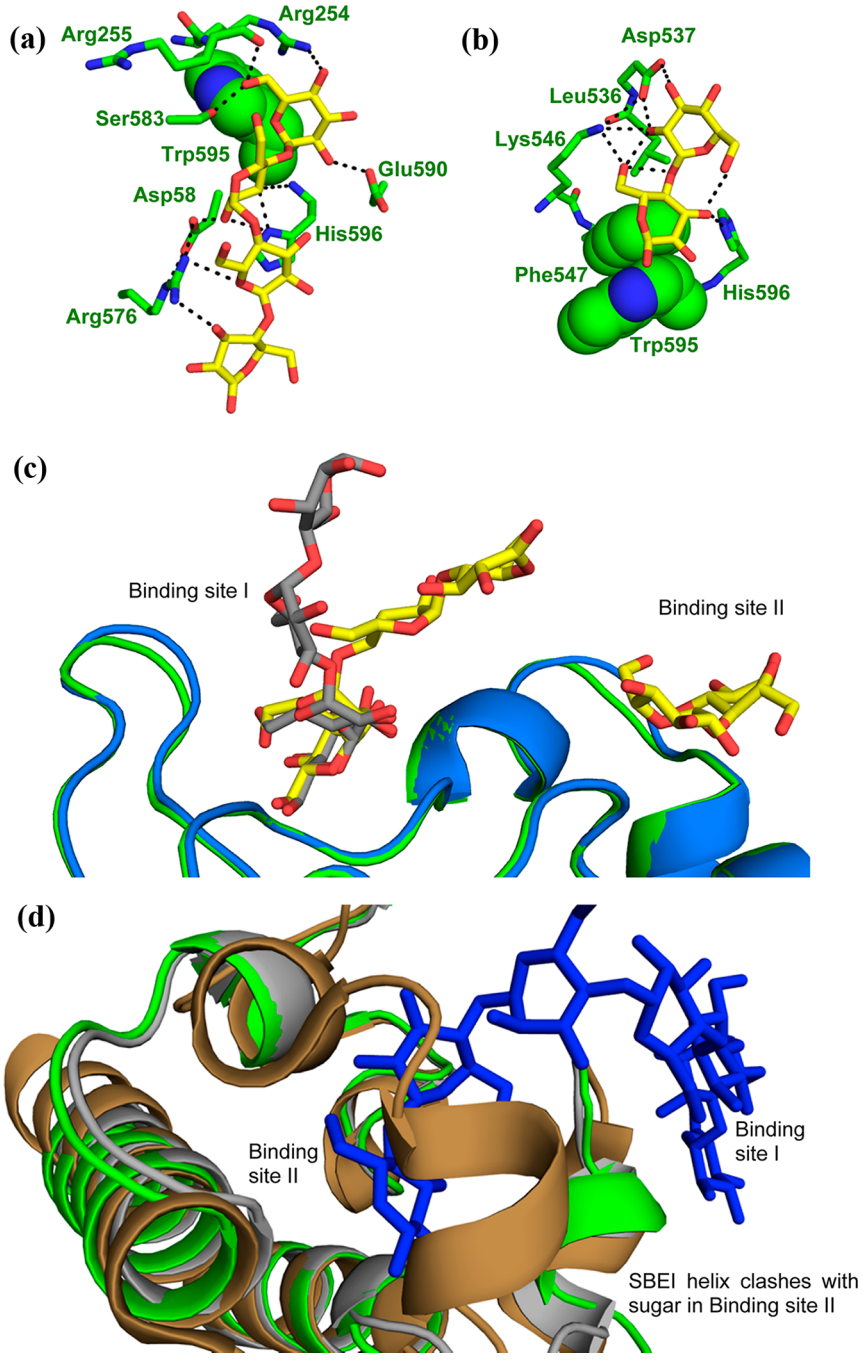

Figure 2. Maltoheptaose binds to *E. coli* BE at binding sites I and II. (a) The nonreducing end of M7 binds to binding site I, and (b) the reducing end binds to binding site II. Protein atoms are colored by type, with C colored green, N colored blue, and O colored red. M7 atoms are also colored by atom type, with C colored yellow and the rest as described above. Dotted black lines show hydrogen bonds. Glucose units of M7 are numbered in red. (c) Overlay of EcBE, molecules B and D (blue). M7 bound to B is colored yellow and to D (only four glucose units are visible) in gray. The first two glucose units of both sugars superimpose, while the rest point away from the surface in molecule D and loop around the molecule to bind to binding site II in molecule B. Residues making hydrophobic interactions are shown as space filling, and residues making hydrogen bonds are shown as sticks in both panels a and b. (d) Overlay of EcBE (green), MtBE (gray), and SBEI (sand) structures (PDB entries 3Q9R, 3K1D, and 3AMK, respectively). The M7 sugar, colored here deep blue to highlight differences in structures in this region (please do not confuse with molecule D in a lighter blue in panel (c)), bound to binding site II, clashes with the short helix of SBEI, proving that the plant enzymes do not bind oligosaccharides at this location.

ordered in molecule A, where a third glucose unit is visible in the electron density. Hydrogen bonds are made between the glucan and the main chain and side chain of Thr508. The glucan is sandwiched among three hydrophobic residues, Leu512 on the top and Trp628 and Phe509 on the bottom of the glucan. It is notable that all six binding sites involve a hydrophobic interaction between a tryptophan aromatic group and a sugar residue.

Biochemical Characterization of EcBE Glucan Binding Sites. In an effort to begin to probe the functional importance of the external binding sites in EcBE discovered in these structures, several residues found to interact with the glucan

DOI: 10.1021/acs.biochem.5b00228
Biochemistry 2015, 54, 6207−6218

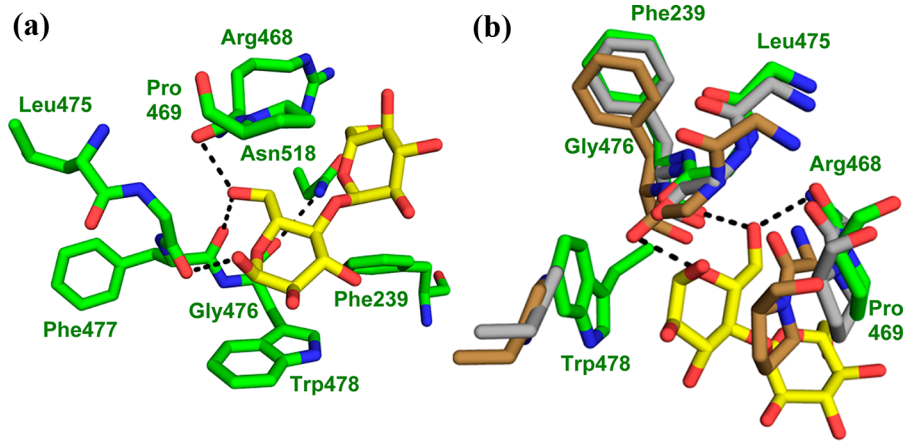

Figure 3. Oligosaccharide binding in binding site III. (a) The detailed interactions between M7 and EcBE at binding site III are shown. Coloring is as in Figure 2a. (b) Overlay of the conserved residues in binding site III of EcBE with MtBE and SBEI (coloring is as in Figure 2c). This figure shows how His453 (MtBE) and His388 (SBEI) stack against the sugar as Trp478 of EcBE does.

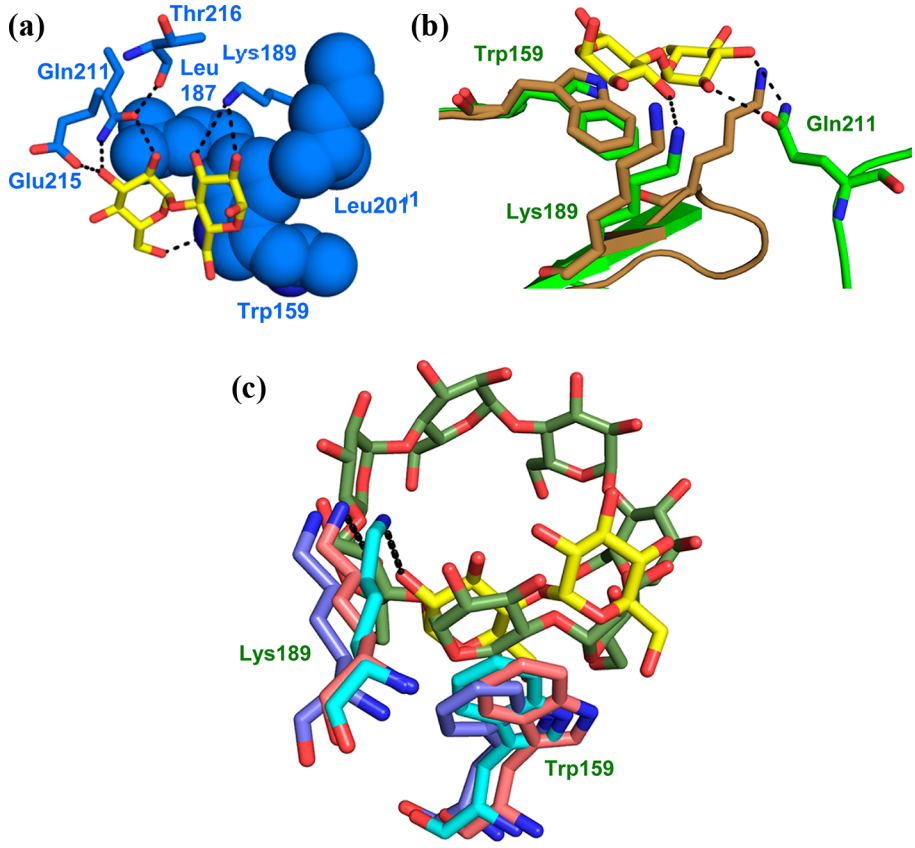

Figure 4. Oligosaccharide binding in binding site IV. (a) The detailed interactions between M7 and molecule D of EcBE (C colored blue, O colored red, and N colored deep blue) at binding site IV. Trp159 stacks against the sugar, making close hydrophobic interactions; two other residues, Leu187 and Leu201, are located in the proximity of the sugar. Hydrogen bonds are shown as dotted black lines. Residues making hydrophobic interactions are shown in space-filling mode, and residues making hydrogen bonds are shown as sticks. (b) Overlay of EcBE (green) and SBEI (sand) showing the conserved residues Trp159 and Lys189 (EcBE numbering). Gln211 (EcBE) and Lys121 (SBEI) occupy close positions, which makes Lys121 potentially able to make a hydrogen bond with the sugar as Gln211 does. (c) Overlay of the CBM48 binding sites of EcBE, AMPK, and DSP4 (PDB entry 4PYH) showing that the two conserved residues, Trp159 and Lys189 (EcBE numbering), make similar interactions with the glucans, despite large differences in the three structures. EcBE is colored cyan, DSP4 slate, and AMPK red.

were mutated in several of the binding sites and the mutants were assayed using an amylose substrate. Table 4 summarizes the results of these studies. The focus was directed at sites I, II, and VI because of their proximity and relative orientation to the active site and, in the case of site VI, the considerably strong degree of amino acid conservation of this sites among branching enzymes. Both the wild-type full-length and truncated *E. coli* branching enzyme were assayed. As shown, while mutations in sites I and VI significantly compromised the activity of the enzyme, mutations to site II had a far weaker effect on activity.

DOI: 10.1021/acs.biochem.5b00228
Biochemistry 2015, 54, 6207−6218

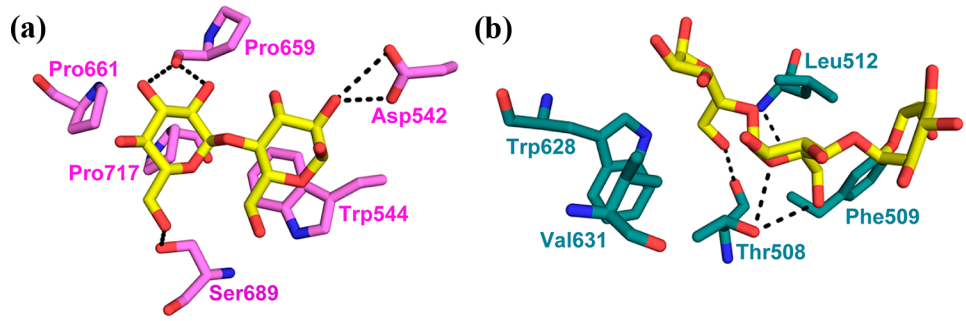

Figure 5. Detailed interactions in binding sites V and VI. (a) Binding site V, where black dotted lines indicate hydrogen bonds, glucan carbons are colored yellow, and EcBE (molecule C) carbons are colored violet. (b) Binding site VI colored as described above but with EcBE (molecule A) carbons colored deep teal.

Table 4. Percent Activities for Binding Site I, II, and VI Mutants

		% activity[a]	
binding site	mutant	WT	Δ-112
I	D585K	16 ± 1.8	32 ± 4.9
	D585A	68 ± 2.9	122 ± 4.7
	R576A	109 ± 5.4	89 ± 4.7
II	D537A	76 ± 3.8	53 ± 2.8
	D537K	126 ± 1.4	160 ± 2.8
	K546A	121 ± 4.0	152 ± 1.9
	W595L	155 ± 1.8	58 ± 3.6
VI	W628A	37 ± 1.3	7 ± 0.62
	W628R	14 ± 1.2	6 ± 0.1

[a]Activity was measured by the iodine stain assay with amylose as the substrate, and percentages were calculated on the basis of WT or Δ-112 activity.

Notably, while the D585A mutation[37] has no effect on the activity of EcBE and only a small effect on the activity of *wt*EcBE, the D585K mutant retained only 32% of the native EcBE activity, and 16% in the full-length enzyme. As shown, this residue makes a direct interaction with G2 of the glucan and in addition orients the R576 side chain, which also makes an interaction with the glucan in site I. A Lys at position 585 is likely to force the R576 out of the binding pocket, leading to the loss of both interactions in the D585K mutant, and thus a much stronger effect on binding. Consistent with the idea that disruption of both contacts is necessary for loss of activity, the R576A mutant retains full activity in both the truncated and full-length enzymes. D585 is strongly conserved in bacterial branching enzymes and is a Gln in the plant enzymes (Figure S2). Together, these data strongly implicate site I to be important for the activity of *E. coli* BE and may be a glucan binding site in both bacterial and eukaryotic enzymes, though binding at this position was not seen in the maltopentaose-bound SBEI structure.

Mutations to site VI had an almost equally debilitating effect on the enzyme's activity. The W628A and W628R mutants both had substantially reduced activity in both the full-length and truncated enzymes. Trp628 is responsible for a side-on hydrophobic interaction with maltoheptaose, and mutation of either Ala or Arg is expected to seriously compromise this interaction. This residue is identical in virtually all bacterial BEs. This indicates that site VI, located on the reducing-end side of the active site, is also important for the activity of EcBE and may be a conserved glucan binding site in bacterial BEs. Together, these data indicate that two of the six external binding sites play important roles in the activity of EcBE.

The Difference between EcBE and Other GH13 Enzymes around the Active Site. In contrast to other GH13 enzymes, no binding is seen in the active site of EcBE, even when six other binding sites were located on the enzyme surface. An analogous result was obtained in the case of a rice BE inactive mutant, where cocrystallization with maltopentaose identified three oligosaccharide binding sites, none of them near the active site of the enzyme.[39] To better understand this difference, we have compared the structure of EcBE with those of all the GH13 enzymes whose structures with glucans bound in the active site have been reported. In all cases, loops emanating from around the active site make numerous contacts with the bound glucan just outside of the active site. These have been described as "subsite binding sites" and are seen in virtually all of the known complexes.[24,26,54−64] In contrast, EcBE has little if any structure in the substrate binding regions found in the other enzymes. In short, it appears that the typical substrate binding motifs found in most GH13 enzymes whose structures are known are not found in EcBE. Though these regions can differ substantially in these enzymes, depending on their substrate and product specificities, they all contain structure in the region around the active site. EcBE is novel in that it is devoid of structure in these regions, indicating that the manner in which it binds its substrates is distinct from those of most members of the GH13 family. It is important to reiterate, however, that the residues that interact with the two sugars in the active site are conserved in all these enzymes as they are in EcBE. We show this by modeling acarbose from the mammalian α-amylase/acarbose structure (PDB entry 1PPI) in the active site of EcBE, showing that the active site residues are conserved (Figure 6a and Figure S2).

As an illustration of the differences between EcBE and other GH13 enzymes in the vicinity of the active site, the structures of apo EcBE (PDB entry 1M7X) and malto-oligosaccharide-bound pig pancreatic α-amylase (PDB entry 1UA3) were overlaid (Figure 6b). As shown, there are significant differences in the structures of the two enzymes in the vicinity of the substrate. In particular, a critical substrate binding loop in α-amylase, which makes both hydrophobic and hydrogen bonding contacts (via Val163), is much shorter in EcBE (the loop from residue 360 to 372 in EcBE is from residue 138 to 164 in α-amylase) and points away from the active site. This loop is involved in substrate contacts in almost all GH13 enzymes whose substrate-bound structures are known. These include cyclodextrin glucanotransferase (PDB entry 1EO5),[27] β-amylase (PDB entry 3BC9),[26] pullulanases (PDB entries

DOI: 10.1021/acs.biochem.5b00228
Biochemistry 2015, 54, 6207−6218

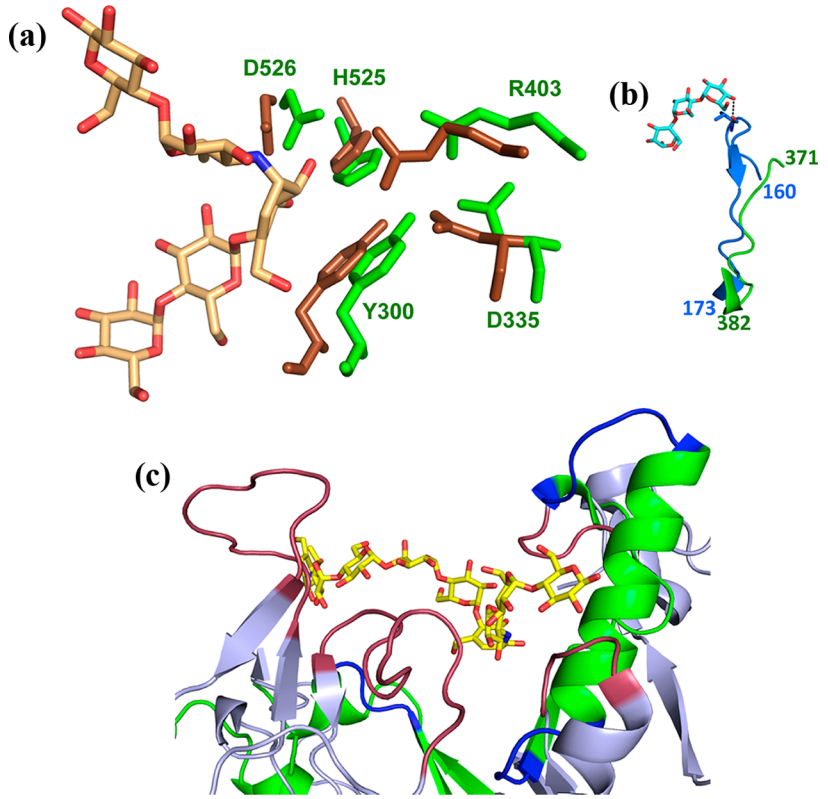

Figure 6. Active site of BE vs the active sites of other GH13 enzymes. (a) Overlay of catalytic residues of EcBE (green) and mammalian α-amylase (PDB entry 1PPI, brown) showing that the catalytic residues in EcBE are conserved, allowing the enzyme to bind oligosaccharides in the active site using equivalent interacting residues as in other GH13 enzymes. The residues are labeled according to EcBE numbering. The acarbose molecule bound to mammalian α-amylase is colored light orange. (b) The structures of EcBE (molecule B, green) and α-amylase from pig pancreas (PDB entry 1UA3, blue) were overlaid. Maltotriose from this structure is shown, with carbons colored yellow and oxygens colored red. The regions encompassing residues Ser360−Thr372 in EcBE and Cys160−Asp173 in 1UA3 are shown and demonstrate how the much shorter loop in EcBE prevents it from interacting with the sugar as residues in the α-amylase do. (c) Another example of an α-amylase (maltohexaose producing α-amylase with a much longer maltononaose, PDB entry 1WPC, cartoon colored blue white and interacting loops colored raspberry) overlaid on EcBE (cartoon colored green and analogue loops colored blue) shows how the loops in the latter are much shorter, if they exist, making the catalytic domain more open around the active site.

2E8Z and 3FAX),[24] neopullulanase (PDB entry 1JL8),[64] sucrose hydrolase (PDB entry 3CZ6),[56] and debranching enzyme (PDB entry 2WC7).[54] In all cases, this loop is substantially longer than it is in EcBE and is in a conformation that essentially closes on the active site to make substrate interactions.

In another example, the maltohexaose producing amylase (PDB entry 1WPC)[55] has four loops pointing toward the pseudo-malto-oligosaccharide ligand (165−177, 191−204, 267−271, and 338−342), while EcBE has either much shorter loops in equivalent positions or no counterpart to the amylase structure (Figure 6c). Together, these comparisons show that while the other GH13 enzymes can be quite different in their substrate binding and local environment around the active site, EcBE is unique in that the active site is very open and shares none of the substrate binding determinants of the other enzymes in the family, with the exception of those required for catalysis.

DISCUSSION

Similar external binding sites have been observed in other GH13 enzymes.[62,65] In an elegant series of experiments, external binding sites were shown to have functional significance in the case of barley α-amylase.[66] However, M7-bound EcBE is unusual in that it contains six distinct glucan binding sites distributed over most of the protein surface (by distinct we mean each site is bound by a single M7 molecule). None of the other GH13 enzymes have as many distributed binding sites, and as discussed before, the active site is usually also occupied by a glucan in these structures.

None of the binding sites are particularly close to the active site of EcBE. The two closest binding sites, binding site I and binding site III, are approximately 18 and 23 Å from the active site (-OH of the Tyr300 residue), respectively. Because the active site is unobstructed by crystal packing in all four molecules in the asymmetric unit (with the nearest symmetry mate >20 Å from any of the four active sites in the asymmetric unit), it would appear that the active site itself may have less affinity for the glucans used in this study than do the external binding sites. For the most part, the oligosaccharide binding sites are relatively far from each other, as well, with the shortest distance between any binding site being 8.4 Å between binding site II and binding site V (the distance between the CA atoms of Trp595 and Trp544 residues). This seems to indicate that EcBE interacts with its substrate sporadically, over relatively large distances. This would prevent the enzyme from having significant activity with shorter substrates, precluding EcBE from transferring short chains to relatively small polymers. This is consistent with the biochemical data that indicate that EcBE

DOI: 10.1021/acs.biochem.5b00228
Biochemistry 2015, 54, 6207−6218

acts on only long polymers to transfer chains no shorter than six units and prefers chains eight or more sugars in length.[36]

A Model for Substrate Recognition in EcBE. The feature that distinguishes BE from virtually all other GH13 enzymes is that it has little if any reactivity or binding affinity for shorter chain glucans. BE reactivity is seen with only large polymers such as glycogen or amylose. In addition, EcBE transfers no chains shorter than five residues and has a strong preference for chains 10−12 units in length.[34] Therefore, EcBE must somehow avoid the typical reactivity of GH13 enzymes, which is either to hydrolyze or to transfer relatively short glucan chains, while having a very similar active site. One way to deal with this problem would be to distribute the substrate binding determinants in space such that only comparatively long glucans would be able to simultaneously occupy both one or more external binding sites and the active site. Shorter oligosaccharides would not have sufficient binding affinity for the enzyme and would therefore be very poor substrates compared to longer glucans. If such a mechanism were used for EcBE, the various external binding sites identified in this study may have distinct functions. For example, binding sites I, II, and IV are relatively well positioned to bind the nonreducing end of a glucan entering the active site, while binding sites III and VI are better positioned to bind the reducing end of a glucan as it exits the active site. The fact that both a donor glucan, which will be cleaved to yield the transferring chain, and an acceptor glucan, which will be branched at one of its α-1,6 positions, must bind may explain the relatively large number of external binding sites in EcBE. One possible model is that the two binding sites on the reducing end of the active site (sites III and VI) each bind either the donor or acceptor glucan. Two of the binding sites on the nonreducing end (binding sites I, II, and IV) might then be responsible for binding the nonreducing ends of the donor and acceptor glucans. The comparative insensitivity to mutation of binding site II makes it the less likely candidate to play this role. On the other hand, the external binding sites may simply be for the purpose of localizing the enzyme on the surface of its polymeric substrate. Further mutagenesis, a variety of assays (activity and chain transfer-length specificity assays, for example), and structural studies of mutant enzyme glucan complexes will be required to understand the role of these external binding sites.

The most surprising result from these structures was that though six external glucan binding sites were identified on the surface of EcBE, none of them are near the active site of the enzyme. This observation was consistent with the fact that the loops that make up glucan subsite binding sites in all other GH13 enzymes were essentially absent in EcBE, indicating a lack of interaction between the enzyme and the sugar units in subsites −1, −2, and −3 and +1, + 2, and +3. This is all consistent with the fact that branching enzymes have shown virtually no reactivity with short glucan substrates, and that *E. coli* BE transfers chains no shorter than six glucose units. We have also shown that mutation of binding sites I and VI leads to significant loss of activity of the enzyme, indicating that external binding sites, disparate from the active site, are nevertheless of central importance to the activity of the enzyme.

■ ASSOCIATED CONTENT

Supporting Information

The Supporting Information is available free of charge on the ACS Publications website at DOI: 10.1021/acs.biochem.5b00228.

One figure showing the electron density associated with the sugar binding at each binding site and another figure illustrating the conservation among species BEs with a sequence alignment (PDF)

■ AUTHOR INFORMATION

Corresponding Author

*Department of Chemistry, Michigan State University, 578 S. Shaw Ln., East Lansing, MI 48824. Telephone: +1 517 355 9715, ext. 234. Fax: +1 517 353 1793. E-mail: geiger@chemistry.msu.edu.

Present Address

§L.F.: Center for Retrovirus Research, College of Pharmacy, The Ohio State University, Columbus, OH 43210.

Funding

We gratefully acknowledge the Department of Energy, Office of Science, Basic Energy Sciences, Chemical Sciences, Geosciences and Biosciences Division (DE-FG02-06ER15822).

Notes

The authors declare no competing financial interest.

■ ACKNOWLEDGMENTS

Use of the Advanced Photon Source was supported by the U.S. Department of Energy, Office of Science, Office of Basic Energy Sciences, under Contract DE-AC02-06CH11357. Use of LS-CAT Sector 21 was supported by the Michigan Economic Development Corp. and the Michigan Technology Tri-Corridor for the support of this research program (Grant 085P1000817). We are thankful to Professor Jack Preiss for providing the *wt*EcBE and EcBE plasmids and development of the iodine stain activity assay.

■ ABBREVIATIONS

AMP, adenosine monophosphate; BE, branching enzyme; BME, mercaptoethanol; CBM48, carbohydrate binding module 48 domain; CGTase, cyclodextrin glucanotransferase; EcBE, *E. coli* branching enzyme truncated at amino acid 112; GH, glycoside hydrolase; IPTG, isopropyl β-D-1-thiogalactopyranoside; M7, maltoheptaose; M6, maltohexaose; MtBE, *Mycobacterium tuberculosis* branching enzyme; *wt*EcBE, wild-type *E. coli* branching enzyme.

■ REFERENCES

(1) Jobling, S. (2004) Improving starch for food and industrial applications. *Curr. Opin. Plant Biol. 7*, 210−218.

(2) Bligh, J., and Frances, H. (1999) Genetic Manipulation of Starch Biosynthesis: Progress and Potential. *Biotechnol. Genet. Eng. Rev. 16*, 177−202.

(3) Preiss, J., Ball, K., Smith-White, B., Iglesias, A. A., Kakefuda, G., and Li, L. (1991) Starch Biosynthesis and its Regulation. *Biochem. Soc. Trans. 19*, 539−547.

(4) Preiss, J., Bloom, M., Morell, M. K., Knowles, V. L., Plaxton, W. C., Okita, T. W., Larsen, R., Harmon, A. C., and Putnam-Evans, C. (1987) Regulation of starch synthesis: enzymological and genetic studies. *Basic Life Sciences 41*, 133−152.

(5) Preiss, J., Cress, D., Hutny, J., Morell, M. K., Bloom, M., Okita, T. W., and Anderson, J. (1989) Regulation of Starch Synthesis: Biochemical and Genetic Studies. *ACS Symp. Ser. 389*, 84−92.

(6) Slattery, C. J., Kavakli, I. H., and Okita, T. W. (2000) Engineering starch for increased quantity and quality. *Trends Plant Sci. 5*, 291−298.

(7) Spilatro, S. R., and Preiss, J. (1987) Regulation of Starch Synthesis in the Bundle Sheath and Mesophyll of *Zea mays L.*: Intercellular Compartmentalization of Enzymes of Starch Metabolism

DOI: 10.1021/acs.biochem.5b00228
Biochemistry 2015, 54, 6207−6218

and the Properties of ADP-Glucose Pyrophosphorylases. *Plant Physiol. 83*, 621−627.
(8) Nakamura, Y., Utsumi, Y., Sawada, T., Aihara, S., Utsumi, C., Yoshida, M., and Kitamura, S. (2010) Characterization of the reactions of Starch Branching Enzymes from rice endosperm. *Plant Cell Physiol. 51*, 776−794.
(9) Boyer, C. D., and Preiss, J. (1981) Evidence for Independent Genetic Control of the Multiple Forms of Maize Endosperm Branching Enzymes and Starch Synthases. *Plant Physiol. 67*, 1141−1145.
(10) Gao, M., Fisher, D. K., Kim, K. N., Shannon, J. C., and Guiltinan, M. J. (1996) Evolutionary conservation and expression patterns of maize Starch Branching Enzyme I and IIb genes suggests isoform specialization. *Plant Mol. Biol. 30*, 1223−1232.
(11) Gao, M., Fisher, D. K., Kim, K. N., Shannon, J. C., and Guiltinan, M. J. (1997) Indepenent Genetic Control of Maize Starch-Branching Enzymes IIa and IIb: Isolation and characterization of SBEIIa cDNA. *Plant Physicology 114*, 69−78.
(12) Guan, H. P., and Preiss, J. (1993) Differentiation of the Properties of the Branching Isozymes from Maize (Zea mays). *Plant Physiol. 102*, 1269−1273.
(13) Tetlow, I. J., and Emes, M. J. (2014) A Review of Starch-branching Enzymes and Their Role in Amylopectin Biosynthesis. *IUBMB Life 66*, 546−558.
(14) Takeda, Y., Guan, H. P., and Preiss, J. (1993) Branching of amylose by the branching isoenzymes of maize endosperm. *Carbohydr. Res. 240*, 253−263.
(15) Guan, H. P., Kuriki, T., Sivak, M., and Preiss, J. (1995) Maize Branching Enzyme Catalyzes synthesis of Glycogen-like Polysaccharide in GlgB-Deficient *Escherichia coli*. *Proc. Natl. Acad. Sci. U. S. A. 92*, 964−967.
(16) Palomo, M., Kralj, S., van der Maarel, M. J., and Dijkhuizen, L. (2009) The unique branching patterns of *Deinococcus* Glycogen Branching Enzymes are determined by their N-terminal domains. *Applied and environmental microbiology 75*, 1355−1362.
(17) Holmes, E., Boyer, C. D., and Preiss, J. (1982) Immunological Characterization of *Escherichia coli* B Glycogen Synthase and Branching Enzyme and Comparison with Enzymes from Other Bacteria. *J. Bacteriol. 151*, 1444−1453.
(18) Murakami, T., Kanai, T., Takata, H., Kuriki, T., and Imanaka, T. (2006) A novel Branching Enzyme of the GH-57 family in the hyperthermophilic archaeon *Thermococcus kodakaraensis* KOD1. *J. Bacteriol. 188*, 5915−5924.
(19) Preiss, J. (1984) Bacterial Glycogen Synthesis and Its Regulation. *Annu. Rev. Microbiol. 38*, 419−458.
(20) Seibold, G. M., Breitinger, K. J., Kempkes, R., Both, L., Kramer, M., Dempf, S., and Eikmanns, B. J. (2011) The glgB-encoded Glycogen Branching Enzyme is essential for glycogen accumulation in *Corynebacterium glutamicum*. *Microbiology 157*, 3243−3251.
(21) Wang, L., and Wise, M. J. (2011) Glycogen with short average chain length enhances bacterial durability. *Naturwissenschaften 98*, 719−729.
(22) Cantarel, B. L., Coutinho, P. M., Rancurel, C., Bernard, T., Lombard, V., and Henrissat, B. (2009) The Carbohydrate-Active EnZymes database (CAZy): an expert resource for Glycogenomics. *Nucleic Acids Res. 37*, D233−238.
(23) Coutinho, P. M., Deleury, E., Davies, G. J., and Henrissat, B. (2003) An Evolving Hierarchical Family Classification for Glycosyltransferases. *J. Mol. Biol. 328*, 307−317.
(24) Gourlay, L. J., Santi, I., Pezzicoli, A., Grandi, G., Soriani, M., and Bolognesi, M. (2009) Group B streptococcus pullulanase crystal structures in the context of a novel strategy for vaccine development. *J. Bacteriol. 191*, 3544−3552.
(25) Stam, M. R., Danchin, E. G., Rancurel, C., Coutinho, P. M., and Henrissat, B. (2006) Dividing the large glycoside hydrolase family 13 into subfamilies: towards improved functional annotations of alpha-amylase-related proteins. *Protein Eng., Des. Sel. 19*, 555−562.
(26) Tan, T. C., Mijts, B. N., Swaminathan, K., Patel, B. K., and Divne, C. (2008) Crystal structure of the polyextremophilic alpha-amylase AmyB from *Halothermothrix orenii*: details of a productive enzyme-substrate complex and an N-domain with a role in binding raw starch. *J. Mol. Biol. 378*, 852−870.
(27) Uitdehaag, J. C. M., van Alebeek, G. J., Van Der Veen, B., Dijkhuizen, L., and Dijkstra, B. W. (2000) Structures of Maltohexaose and Maltoheptaose Bound at the Donor Sites of Cyclodextrin Glycosyltransferase Give Insight into the Mechanisms of Transglycosylation Activity and Cyclodextrin Size Specificity. *Biochemistry 39*, 7772−7780.
(28) Woo, E. J., Lee, S., Cha, H., Park, J. T., Yoon, S. M., Song, H. N., and Park, K. H. (2008) Structural insight into the bifunctional mechanism of the glycogen-debranching enzyme TreX from the archaeon *Sulfolobus solfataricus*. *J. Biol. Chem. 283*, 28641−28648.
(29) Santos, C. R., Tonoli, C. C., Trindade, D. M., Betzel, C., Takata, H., Kuriki, T., Kanai, T., Imanaka, T., Arni, R. K., and Murakami, M. T. (2011) Structural basis for Branching-Enzyme activity of glycoside hydrolase family 57: structure and stability studies of a novel Branching Enzyme from the hyperthermophilic archaeon *Thermococcus kodakaraensis* KOD1. *Proteins: Struct., Funct., Genet. 79*, 547−557.
(30) Kuriki, T., and Imanaka, T. (1999) The Concept of the Alpha-Amylase Family: Structural Similarity and Common Catalytic Mechanism. *J. Biosci. Bioeng. 87*, 557−565.
(31) Chiba, S. (1997) Molecular mechanism in alpha-glucosidase and glucoamylase. *Biosci., Biotechnol., Biochem. 61*, 1233−1239.
(32) Sinnott, M. L. (1990) Catalytic Mechanisms of Enzymic Glycosyl Transfer. *Chem. Rev. 90*, 1171−1202.
(33) Kelly, R. M., Leemhuis, H., and Dijkhuizen, L. (2007) Conversion of a Cyclodextrin Glucanotransferase into an Alpha-Amylase: Assessment of Directed Evolution Strategies. *Biochemistry 46*, 11216−11222.
(34) Binderup, K., Mikkelsen, R., and Preiss, J. (2002) Truncation of the amino terminus of Branching Enzyme changes its chain transfer pattern. *Arch. Biochem. Biophys. 397*, 279−285.
(35) Devillers, C. H., Piper, M. E., Ballicora, M. A., and Preiss, J. (2003) Characterization of the branching patterns of Glycogen Branching Enzyme truncated on the N-terminus. *Arch. Biochem. Biophys. 418*, 34−38.
(36) Binderup, K., Mikkelsen, R., and Preiss, J. (2000) Limited proteolysis of Branching Enzyme from *Escherichia coli*. *Arch. Biochem. Biophys. 377*, 366−371.
(37) Abad, M. C., Binderup, K., Rios-Steiner, J., Arni, R. K., Preiss, J., and Geiger, J. H. (2002) The X-ray crystallographic structure of *Escherichia coli* Branching Enzyme. *J. Biol. Chem. 277*, 42164−42170.
(38) Pal, K., Kumar, S., Sharma, S., Garg, S. K., Alam, M. S., Xu, H. E., Agrawal, P., and Swaminathan, K. (2010) Crystal structure of full-length *Mycobacterium tuberculosis* H37Rv Glycogen Branching Enzyme: insights of N-terminal beta-sandwich in substrate specificity and enzymatic activity. *J. Biol. Chem. 285*, 20897−20903.
(39) Haworth, W. N., Hirst, E. L., and Isherwood, E. (1937) Polysaccharides. Part XXIII. Determination of the Chain Length of Glycogen. *J. Chem. Soc.*, 577−581.
(40) Noguchi, J., Chaen, K., Vu, N. T., Akasaka, T., Shimada, H., Nakashima, T., Nishi, A., Satoh, H., Omori, T., Kakuta, Y., and Kimura, M. (2011) Crystal structure of the Branching Enzyme I (BEI) from *Oryza sativa* L with implications for catalysis and susbtrate binding. *Glycobiology 21*, 1108−1116.
(41) Guan, H., Li, P., Imparl-Radosevich, J., Preiss, J., and Keeling, P. (1997) Comparing the Properties of *Escherichia coli* Branching Enzyme and Maize Branching Enzyme. *Arch. Biochem. Biophys. 342*, 92−98.
(42) Mossessova, E., and Lima, C. D. (2000) Ulp1-SUMO Crystal Structure and Genetic Analysis Reveal Conserved Interactions and a Regulatory Element Essential for Cell Growth in Yeast. *Mol. Cell 5*, 865−876.
(43) Otwinowski, Z., and Minor, W. (1997) Processing of X-Ray Diffraction Data Collected in Oscillation Mode. *Methods Enzymol. 276*, 307−326.

DOI: 10.1021/acs.biochem.5b00228
Biochemistry 2015, 54, 6207−6218

(44) Collaborative Computational Project, Number 4 (1994) The CCP4 suite: programs for protein crystallography. *Acta Crystallogr., Sect. D: Biol. Crystallogr. D50*, 760−763.
(45) Boyer, C. D., and Preiss, J. (1978) Multiple Forms of (1,4)-alpha-D-Glucan, (1,4)-alpha-D-Glucan-6-Glycosyl Transferase From Developing *Zea mays L.* Kernels. *Carbohydr. Res. 61*, 321−334.
(46) Larson, S. B., Day, J. S., and McPherson, A. (2010) X-ray crystallographic analyses of pig pancreatic alpha-amylase with limit dextrin, oligosaccharide, and alpha-cyclodextrin. *Biochemistry 49*, 3101−3115.
(47) Mikami, B., Iwamoto, H., Malle, D., Yoon, H. J., Demirkan-Sarikaya, E., Mezaki, Y., and Katsuya, Y. (2006) Crystal structure of pullulanase: evidence for parallel binding of oligosaccharides in the active site. *J. Mol. Biol. 359*, 690−707.
(48) Okazaki, N., Tamada, T., Feese, M. D., Kato, M., Miura, Y., Komeda, T., Kobayashi, K., Kondo, K., Blaber, M., and Kuroki, R. (2012) Substrate recognition mechanism of a glycosyltrehalose trehalohydrolase from *Sulfolobus solfataricus* KM1. *Protein science: a publication of the Protein Society 21*, 539−552.
(49) Uitdehaag, J. C. M., Mosi, R., Kalk, K. H., van der Veen, B., Dijkhuizen, L., Withers, S. G., and Dijkstra, B. W. (1999) X-ray structures along the reaction pathway of cyclodextrin glycosyltransferase elucidate catalysis in the a-amylase family. *Nat. Struct. Biol. 6*, 432−436.
(50) Glaser, F., Pupko, T., Paz, I., Bell, R. E., Bechor-Shental, D., Martz, E., and Ben-Tal, N. (2003) ConSurf: Identification of Functional Regions in Proteins by Surface-Mapping of Phylogenetic Information. *Bioinformatics 19*, 163−164.
(51) Asensio, J. L., Ardá, A., Cañada, F. J., and Jiménez-Barbero, J. (2013) Carbohydrate - Aromatic Interactions. *Acc. Chem. Res. 46*, 946−954.
(52) Meekins, D. A., Raththagala, M., Husodo, S., White, C. J., Guo, H. F., Kotting, O., Vander Kooi, C. W., and Gentry, M. S. (2014) Phosphoglucan-bound structure of starch phosphatase Starch Excess4 reveals the mechanism for C6 specificity. *Proc. Natl. Acad. Sci. U. S. A. 111*, 7272−7277.
(53) Illingworth, B., Larner, J., and Cori, G. T. (1952) Structure of Glycogens and Amylopectins-I. Enzymatic Determination of Chain Length. *J. Biol. Chem. 199*, 631−640.
(54) Dumbrepatil, A. B., Choi, J. H., Park, J. T., Kim, M. J., Kim, T. J., Woo, E. J., and Park, K. H. (2010) Structural features of the Nostoc punctiforme debranching enzyme reveal the basis of its mechanism and substrate specificity. *Proteins: Struct., Funct., Genet. 78*, 348−356.
(55) Kanai, R., Haga, K., Akiba, T., Yamane, K., and Harata, K. (2004) Biochemical and Crystallographic Analyses of Maltohexaose-Producing Amylase from Alkalophilic *Bacillus sp.* 707. *Biochemistry 43*, 14047−14056.
(56) Kim, M. I., Kim, H. S., Jung, J., and Rhee, S. (2008) Crystal structures and mutagenesis of sucrose hydrolase from *Xanthomonas axonopodis pv.* glycines: insight into the exclusively hydrolytic amylosucrase fold. *J. Mol. Biol. 380*, 636−647.
(57) Knegtel, R. M. A., Strokopytov, B., Penninga, D., Faber, O. G., Rozeboom, H. J., Kalk, K. H., Dijkhuizen, L., and Dijkstra, B. W. (1995) Crystallographic Studies of the Interaction of Cyclodextrin Glycosyltransferase from *Bacillus circulans* Strain 251 with Natural Substrates and Products. *J. Biol. Chem. 270*, 29256−29264.
(58) Mikami, B., Adachi, M., Kage, T., Sarikaya, E., Nanmori, T., Shinke, R., and Utsumi, S. (1999) Structure of Raw Starch-Digesting *Bacillus cereus* beta-Amylase Complexed with Maltose. *Biochemistry 38*, 7050−7061.
(59) Nakai, H., Baumann, M. J., Petersen, B. O., Westphal, Y., Hachem, M. A., Dilokpimol, A., Duus, J. O., Schols, H. A., and Svensson, B. (2010) *Aspergillus nidulans* alpha-galactosidase of glycoside hydrolase family 36 catalyses the formation of alpha-galacto-oligosaccharides by transglycosylation. *FEBS J. 277*, 3538−3551.
(60) Payan, F., and Qian, M. (2003) Crystal Structure of the Pig Pancreatic 'Alpha-Amylase Complexed with Malto-Oligosaccharides. *J. Protein Chem. 22*, 275−284.
(61) Qian, M., Haser, R., Buisson, G., Duee, E., and Payan, F. (1994) The Active Center of a Mammalian a-Amylase. Structure of the Complex of a Pancreatic alpha-Amylase with a Carbohydrate Inhibitor Refined to 2.2-A Resolution. *Biochemistry 33*, 6284−6294.
(62) Strokopytov, B., Penninga, D., Rozeboom, H. J., Kalk, K. H., Dijkhuizen, L., and Dijkstra, B. W. (1995) X-ray Structure of Cyclodextrin Glycosyltransferase Complexed with Acarbose. Implications for the Catalytic Mechanism of Glycosidases. *Biochemistry 34*, 2234−2240.
(63) Vester-Christensen, M. B., Abou Hachem, M., Svensson, B., and Henriksen, A. (2010) Crystal structure of an essential enzyme in seed starch degradation: barley limit dextrinase in complex with cyclodextrins. *J. Mol. Biol. 403*, 739−750.
(64) Yokota, T., Tonozuka, T., Shimura, Y., Ichikawa, K., Kamitori, S., and Sakano, Y. (2001) Structures of *Thermoactinomyces vulgaris R-47* alpha-amylase II complexed with substrate analogues. *Biosci., Biotechnol., Biochem. 65*, 619−626.
(65) Robert, X., Haser, R., Gottschalk, T. E., Ratajczak, F., Driguez, H., Svensson, B., and Aghajari, N. (2003) The Structure of Barley α-Amylase Isozyme 1 Reveals a Novel Role of Domain C in Substrate Recognition and Binding. *Structure 11*, 973−984.
(66) Nielsen, M. M., Bozonnet, S., Seo, E. S., Motyan, J. A., Andersen, J. M., Dilokpimol, A., Abou Hachem, M., Gyemant, G., Naested, H., Kandra, L., Sigurskjold, B. W., and Svensson, B. (2009) Two secondary carbohydrate binding sites on the surface of barley alpha-amylase 1 have distinct functions and display synergy in hydrolysis of starch granules. *Biochemistry 48*, 7686−7697.

DOI: 10.1021/acs.biochem.5b00228
Biochemistry 2015, 54, 6207−6218